Bimetallic copper-based nanowires and the means to create next-generation stable transparent electrodes

Anđela Križan, Kevin Zimny, Alexandre Guyonnet, Emmanuel Opeyemi Idowu, Etienne Duguet, Marie Plissonneau, Lauriane D'alençon, Thierry Le Mercier, Mona Tréguer-Delapierre

NANO EXPRESS

TOPICAL REVIEW

Bimetallic copper-based nanowires and the means to create next-generation stable transparent electrodes

Anđela Križan[1], **Kevin Zimny**[1], **Alexandre Guyonnet**[1], **Emmanuel Opeyemi Idowu**[1], **Etienne Duguet**[1], **Marie Plissonneau**[2], **Lauriane d'Alençon**[2], **Thierry Le Mercier**[2] **and Mona Tréguer-Delapierre**[1,*]

[1] Univ. Bordeaux, CNRS, Bordeaux INP, ICMCB, UMR 5026, 33600 Pessac, France
[2] Solvay R&I, 52 rue de la Haie Coq, 93306 Aubervilliers, France
* Author to whom any correspondence should be addressed.

E-mail: mona.treguer@icmcb.cnrs.fr

Keywords: bimetallic, nanowires, copper, transparent electrodes

OPEN ACCESS

RECEIVED
29 July 2023

REVISED
21 September 2023

ACCEPTED FOR PUBLICATION
9 October 2023

PUBLISHED
20 October 2023

Abstract

Metallic nanowire percolating networks are one of the promising alternatives to conventional transparent conducting electrodes. Among the conductive metals, copper appears as a relevant alternative to develop electrodes in a more sustainable and economical way (abundance of the supplies, geo-political risks regarding the supplies, environmental impact, and cost). However, Cu nanowires suffer from high instability in air, and one of the ways to increase stability as well as to boost properties related to transparent electrodes is to combine the Cu with another metal, resulting in bimetallic nanowires. Even though the field of fabrication of nanoalloys has been advancing at a rapid pace in the last two decades, binary nanowires are difficult to produce due to a wide range of parameters that must be aligned in regard to metals that are being combined, such as surface energy of the bulk metal, atomic radii, crystal lattice matching, redox potentials, etc. In this review, we present the current research landscape in making Cu-based bimetallic nanowires for the development of metal nanowire networks with high oxidation resistance. This analysis allows identifying the most promising bimetallic materials for obtaining highly efficient, robust, and cost-effective electrodes.

1. Introduction

Transparent electrodes (TEs) represent an integral component in a wide range of modern-day devices, some of them being solar cells, smart windows, touch screens, Light Emitting Diodes (LEDs), transparent heaters, liquid-crystal displays (LCD) paper-like displays, etc [1–4]. The market for TEs has been evolving exponentially in the past years, with its growth being driven by the need for these devices. Ultimately, it is expected that the global TE market will grow from 1.02 billion USD in 2017 to 2.48 billion USD by 2030, at a compound annual growth rate of 10.5% from 2017 to 2030 [5]. For example, the number of mobile phones is expected to increase at a rate of 6% per year. Naturally, as the demand for such devices increases, so does the demand for novel, more efficient, sustainable, versatile, and cost-friendly materials to produce them. The main parameters required for TEs, as the name suggests, are optical transparency and electrical conductivity. However, in recent years, flexibility has been sought as a favorable parameter as well. Historically, the main constituents of TEs have been transparent conductive oxides (TCOs), most notably SnO_2 and In_2O_3. These wide band-gap semiconductors have intrinsically low absorption of light, making them highly transparent in the visible. Furthermore, doping can be utilized to enhance the conductivity of TCOs. Considering how the research on TCOs began developing around the middle of the past century, these materials have been majorly improved and are generally well understood and can be modified to fit different market needs. Subsequently, in the market today, the most commonly used material for TEs is indium tin oxide (ITO). However, despite the excellent optoelectrical properties of ITO, there are both physical and economic considerations to be made regarding this material. Its ceramic nature expresses itself in high brittleness, deeming ITO non-compatible with growing demands for flexible electronics. In regard to economic considerations, both the production means and the price of indium must be addressed. ITO is prepared by vacuum-deposition tools

that require expensive facilities and intrinsically lead to high power consumption, deeming fabrication costs a yet unresolved issue. Furthermore, ITO is expected to become increasingly expensive due to the scarcity of indium, its price currently standing at 229 \$ kg^{-1}, with its price already increased by more than 13.94% since the beginning of 2023, according to trading on a contract for difference that tracks the benchmark market for this commodity [6]. Considering all this, it is rather obvious why the demand for novel materials for TEs is high and continues to increase. Thus far, three primary categories of alternative materials for TEs have emerged: (1) doped metal oxides such as fluorine-doped tin oxide and aluminium-doped zinc oxide (2) non-metallic nanomaterials (conducting polymers, graphene, carbon nanotubes, etc.), (3) metal-based nanomaterials (metallic nanowire networks (MNWs), metal grids, continuous metallic thin films, oxide/metal/oxide multilayered films, metallic nanofibers) [1–4, 7]. Among these materials, metal NWs represent a very promising candidate as an ITO competitor, as they possess the means to address the previously discussed problems associated with ITO. They are the only material that can both exceed the performance of ITO, and can be coated from solution at rates, even $>$ 100 times faster than sputtering, a coating technique used for ITO [8]. When metallic NWs are assembled into random percolating networks, they can act efficiently as TEs and can be easily integrated into flexible and stretchable devices thanks to their outstanding properties. Metallic nanomaterials possess intrinsically high conductivity, their nanoscale morphology allows high transparency and flexibility, and when combined with other materials, other properties such as haze and bandgap alignment are tunable [9]. Moreover, the anisotropic structure provides charge carrier confinement that leads to one-dimensional ballistic transport of electrons [10]. Additionally, their high aspect ratio ensures a more favorable material/surface ratio as there is no need for the entire surface to be covered for the conductive properties to be exhibited. Only several tens of mg m^{-2} are needed for metal NW networks to be conductive [11]. When it comes to other economic considerations, MNWs provide additional benefits due to simple preparation protocols and no need for high-end equipment. Currently, silver nanowires (Ag NWs) are the most widely studied material for TEs due to their optoelectrical properties in line with those of ITO, the market standard. When Ag NWs are deposited in the form of a thin film by utilizing bottom-up processes (wet chemical synthesis, followed by large-area coating or printing at atmospheric pressure), they combine high electrical conductivity, optical transparency, and bendability. In a typical Ag NW thin film, transparencies over 90% are commonly reported, with sheet resistances of around 10 Ω sq^{-1}. By varying the density of the NW network, it is possible to modify the transparency and conductivity of the films as a function of the targeted applications. However, even though Ag NWs are a cheaper alternative to ITO, silver resources are also limited and this may cause major issues for the TE-scale deployment in the future [12, 13]. Moreover, in 2023, the price for raw Ag lies at 669 $\in$ kg^{-1} [14] and is predicted to continue to rise due to its growing use in industrial settings. For comparison, indium currently lies at 204 $\in$ kg^{-1} [14]. These are the main reasons why other metals are being explored for the preparation of transparent conductors based on NW networks. Copper NWs (Cu NWs) are one of the primary candidates [15–17], as they are 1000 times more abundant than silver (Cu: 7.43 $\in$ kg^{-1} in 2023 [14]), just as inexpensive for preparation, and can be synthesized quickly while retaining desirable optical and electrical properties. Another important factor is the relative atomic mass of copper, which stands at 59% of silver. This aspect is a major benefit when it comes to the production of lightweight devices. However, Cu NWs have a major intrinsic drawback—a lack of thermal and chemical stability [18]. The rapid oxidation of the Cu NWs in air yields the formation of an insulating oxide layer [19]. It causes the conductivity of TEs to deteriorate in a couple of daysdeclining the performance of the opto-electronic devices. Recent studies in the literature have shown that the preparation of bimetallic NWs could be an advantageous solution to tackle this problem. Coating the entire surface of Cu NW networks with polymers, carbon, a metal oxide layer or multilayered materials is also an interesting alternative [20, 21]. However, one of the drawbacks of polymer coatings is that they directly lower the conductivity of the electrodes because of the increased junction resistance between the NWs, given their dielectric nature. The carbon materials negatively affect the structure of the metallic copper, causing the reduction of the conductivity of the electrodes [18]. The oxide layers lead to a much-enhanced thermal and electrical stability along with better adhesion, but this is at the expense of optical transmittance decrease. In this article, we focus on copper-based bimetallic nanowires (CuM NWs). We report the significant progress in the synthesis of these NWs achieved in the past few years to obtain robust composites that could fulfil the increasing demand for flexible TE. We then detail the most relevant methods developed for fabricating transparent conductors using these bimetallic NWs. Finally, we conclude on the key challenges and future directions in this growing field.

2. Copper-based bimetallic nanowires

2.1. General considerations

The interest in bimetallic CuM nanostructures comes from the emergence of specific electronic, optical, and chemical properties, which result not only from the combination of the intrinsic properties of the parent metals, but also from new properties due to synergy between both elements [22]. It is well known that, at the nanoscale,

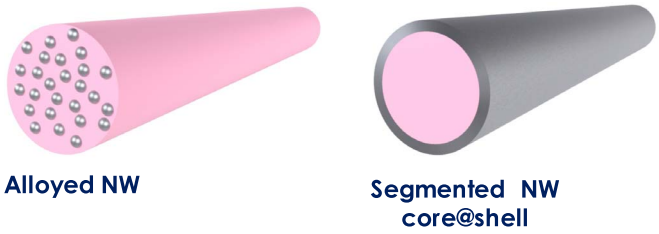

Figure 1. Schematic representation of the most common copper-based bimetallic NWs discussed in this review (Cu (pink), other metal (grey)).

the chemical and physical properties of the nanoalloys are strongly dependent on the precise control of the size, structure, and composition, but also on the relative spatial distribution of the atoms within the nanoparticle (degree of chemical ordering and miscibility). We have represented the most commonly reported structures for CuM NWs in a general scheme shown in figure 1. The major bimetallic architectures typically found in the literature are either alloyed (ordered or random atomic arrangement), or segregated nanostructures (Cu (core) @M (shell) architecture or Janus nanoparticles, the latter isn't discussed in this review).

For the same composition, a change in the atomic arrangement within a 1D nanostructure may induce different physical and chemical properties. For example, it has been observed that small changes in the organization of the metal atoms within the nanostructure can improve the chemical and thermal stability and enhance the electric performances [19, 23, 24]. This effect however, is under-reported in the literature for Cu 1D nanostructures, making it difficult to draw conclusions on the effect of alloying on such Cu based systems. Other than in regard to intrinsic conductivity, the interest of mixing copper with other metals in an alloy is of high interest, and one of the most sought combination is that of Cu and Ag, as it could both suppress the oxidation problem of Cu nanoparticles and reduce the intrinsic cost of Ag nanoparticles.

The formation of alloyed or core@shell architecture is dependent on the miscibility of the two metals and can be predicted by different factors [25–29]:

- The dissociation energy of the metal bonds: miscibility is favored if the heteronuclear metal bonds Cu-M are stronger than the homonuclear Cu-Cu and M-M ones.
- The surface energy of two bulk metals: the element with the lower surface energy tends to segregate on the surface.
- The atomic radius: the smaller atoms tend to form the core of the nanostructure.
- The charge transfer: the electronic transfer of the element with the lowest electronegativity toward the other one favors the miscibility and the alloying.
- The strength of the bonds with the shaping (capping) agents on the NW: the metal that has a strong bond with the ligand (or the substrate) is the one that will be on the surface.
- The redox potential: it dictates the possibility of co-reduction, necessary for the formation of an alloy.

In addition, studies report on some more intricate parameters that drastically impact the viability of bimetallic alloy formation, most notably but not limited to: kinetics versus equilibrium during the synthesis, entropy of the system, strain, and twin boundaries. Thus, the formation of alloys is favored for metals with similar physicochemical parameters (atomic radius, electronegativity, surface energy, redox potential…). Table 1 presents some physico-chemical characteristics of the most promising metals to significantly improve the stability of copper for the considered applications [30–33]. These systems form the basis of the most fabricated and used bimetallic NWs so far. However, their alloying ability within nanostructures of high aspect ratio is difficult to predict and continues to be a major goal of research in alloy systems [28, 34].

2.2. Fabrication of bimetallic nanowires

A wide variety of approaches exist for the bottom-up fabrication of bimetallic NWs. In this section, we provide a brief overview of the most relevant methods developed by chemists. They can be classified into two main categories: (1) simultaneous co-reduction of two kinds of metal ions (one step) (2) successive reduction where Cu core is formed first, followed by the reduction of another metal precursor (multi-step approach), as outlined in figure 2.

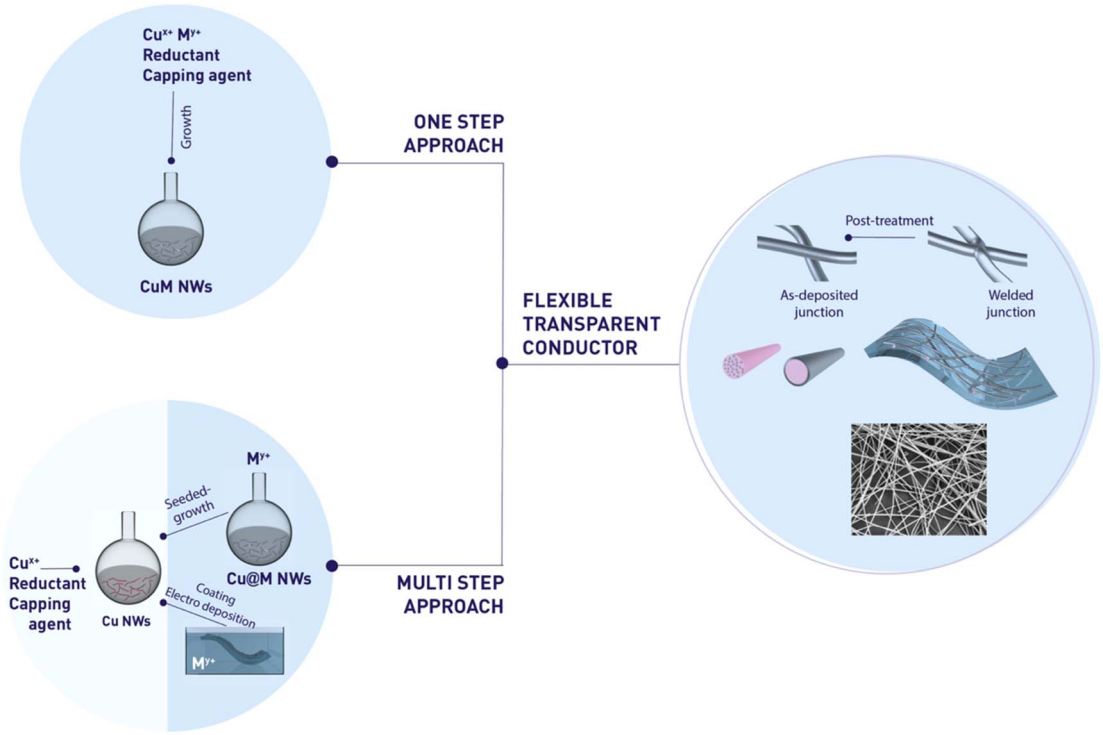

Figure 2. Schematic of most commonly reported approaches for preparing CuM NW-based TEs. The bimetallic NWs are prepared either by a one-step approach or by a multi-step approach, upon which they are deposited onto a flexible substrate, followed by a post-treatment. The post-treatment enables to fuse the wire-wire junction in NW network. Scanning electron microscope image of bimetallic NW network deposited by spray-coating (mean NW diameter: 30 nm).

Table 1. Physico-chemical characteristics of Cu, Ni, Ag, Au, and Sn (fcc is face centered cubic; bct: body centered tetragonal). The data are extracted from [30–33].

	Surface energy ($J.m^{-2}$)	Radius (pm)	Electro-negativity	Cell parameter (pm)	M-M Dissociation energy ($kJ.mol^{-1}$)
Cu	1.8	135	1.90	362 (fcc)	202
Ni	2.4	135	1.91	358 (fcc)	262
Ag	1.2	160	1.93	418 (fcc)	163
Au	1.5	135	2.54	420 (fcc)	222
Sn	0.7	145	1.96	319 (bct)	195

In colloidal synthesis, metal atoms are obtained by chemical reduction or thermal decomposition of metal precursors, i.e. inorganic or organometallic salts. Copper precursors can be easily reduced into metal nuclei due to the high reduction potential of the Cu ion. To promote anisotropic growth of the metal nuclei into NWs, the reduction reaction is achieved in the presence of judiciously chosen shaping /capping agent(s) that bind onto a specific facet of the growing seed crystals, further hindering growth in the direction related to the blocked facet(s). At the end of the synthesis, the nanoparticles are stabilized by the soft corona of shaping/capping agent(s) giving properties like solvation, colloidal stability and surface chemistry. In a large collection of studies, organic amines are employed as shaping agents to synthesize monometallic Cu NWs [35, 36]. Generally, temporal separation of nucleation and growth steps favors the production of NWs with high morphological yield. Cu NWs can also be prepared by electrodeposition into the pore walls of sacrificial porous membranes (aluminium oxide, silicon, and polycarbonate). In such membranes, the pores act as a template for the nano-structuration [35, 37, 38].

To promote the mixing necessary for the formation of an alloyed NW, both metal precursors must be present simultaneously during the nucleation and growth stages to obtain a bimetallic structure (figure 2 top left panel). Their decomposition/reduction profiles should be almost identical to favor the formation of nuclei that contain both metals. The final composition of a NW can be tailored by varying several parameters such as the reduction potential of the metal ion involved, the strength of the reductant, the nature of the coordination ligand, the reaction temperature, the shaping agent, varying the molar ratio of the precursors, *etc.* But, the

Table 2. Review of the reports on CuM (M = Ni, Ag, Au, Sn, Zn) NWs and the achieved composition (alloyed or segmented (core@shell)).

	Segmented NWs	Alloyed NWs	Aspect ratio
CuNi	[45–53, 55, 56, 59–61, 63, 64, 66–68]	[49–52, 54, 57, 58, 62]	20–500 [46–50, 52–54, 56, 57, 59–65, 67, 68] >500 [45, 51, 55, 58, 66]
CuAg	[81–94]	/	10–500 [81–94]
CuAu	[23, 97, 100, 101]	[23, 102]	>500 [23, 97]
CuSn	[106–110]	[105, 109, 110]	10–100 [105, 107, 108]
CuZn	[55, 113, 117–119]	[112–116]	20–500 [117 > 500 [114, 116]

underlying growth processes of the elongated nano-objects are not fully understood, since the reactants can play different roles. In general, two metallic precursors with similar standard redox potentials have a good chance to form a disordered alloyed NW by simultaneous co-reduction in one step. Inversely, two precursors with a large difference in the redox potential are very likely to be combined into a core–shell system. The metal with the highest redox potential nucleates first, forming the core of the particle, followed by the growth of the other metal which prevails at the surface. The composition of the NWs may vary from the core to the periphery, and hence, architectures with a gradient of composition can occur. Utilizing coordinating ligands to form complexes with the metallic cations can also be employed to manipulate the redox potential of precursors and produce a homogeneously mixed solid phase with different metallic couples. In addition to the intrinsic difficulties of synthesizing nanoparticles in which the two metals are intimately bounded, the production of 1D bimetallic nano-objects in high yields poses a challenge as well. This is important to mention, as for TEs, very high aspect ratio nanostructures are of the highest interest. Despite the recent progress in colloidal synthesis, controlling both composition and shape in the meantime remains a huge challenge. Reports of reliable protocols capable of producing real alloyed NWs in one step remain rare. Most of the reports produce NWs with a core@shell architecture (table 2).

The synthesis of core@shell NWs in a controlled manner can be obtained by multi-step colloidal chemistry as well as electrochemical deposition or chemical vapor deposition (figure 2 bottom left panel). The first step involves the synthesis of a template nanoparticle consisting of Cu NWs. This latter can be modified to favor the deposition of another metal. It serves as a physical template for the coating process in aqueous or non-aqueous solvent. As indicated earlier, the synthesis of the copper particles involves the reduction of copper in the presence of a shaping agent. Then, the surface of the template can be chemically modified with functional groups which can enable the conjugation of ions of another metal. Their reduction onto the pre-existing core nuclei leads to the formation of core@shell particles. By tuning the amount of metal precursor added, one can precisely control the shell thickness, given that the deposition is homogeneous and follows a layered growth mode. Robust protocols have thus been developed to allow, most prominently, the growth of Ni, Ag, Au, Sn, etc with a well-defined shell in high yields and quantity.

It is possible to form objects with varied architectures, since galvanic replacement reaction and/or Kirkendal effect can also be exploited to make alloyed, textured nanoshells and/or change the shell composition. The galvanic replacement reaction allows the exchange of some of the copper surface atoms with another metal (a more noble one) by exposing the Cu-template to a salt solution of the other metal M^{x+}, allowing redox chemistry to run its course [39, 40]. The final product depends on the stoichiometry and the oxidation state of the metal precursor M^{x+}. The templates can be covered by a homogeneous shell of one metal, a mixture of metallic elements CuM or a shell containing voids on the surface. In the latter case, the pores are often poorly defined and their positions are randomly distributed across the surface. Having that in mind, while the galvanic replacement can be used to form specific architectures, if uncontrolled, it can also lead to unwanted products. In the case of metals with a large difference in redox potential, the core may be fully replaced at the expense of the galvanic reaction. To avoid the removal of the core due to galvanic replacement, several methods can be applied, such as adding a co-reductant to serve as an alternative source of electrons, modifying the reduction potential of the metal ions, and the use of protective layers.

The Kirkendall effect can also be used to convert the starting Cu NWs into a core@shell nanostructure with a textured and/or porous shell [39, 41]. It refers to the movement of the atoms of metallic species at a bimetallic interface. The phenomenon is observed when one of the two metals has a significantly higher diffusion rate than the other. It can occur, for instance, during galvanic replacement reaction and/or upon annealing treatment. Depending on the diffusion rates of both metallic atoms Cu^0 or M^0, unexpected shell compositions and configurations can be formed. The atomic movement can lead to voids (Kirkendall voidening), and/or alloying

due to interdiffusion. Finally, repeated occurrence of the Kirkendall effect can result in a generation of multilayered core@shell nanostructures.

Core@shell nanostructures can also be prepared by electrodeposition (figure 2 bottom left panel). The Cu NW templates deposited on a side of a given substrate can be used as nanoelectrodes to produce the CuM NWs. The reduction of another metal species onto the pre-deposited Cu NWs can take place by applying an external current output. Given the great enough difference in the redox potentials of the metal species, a galvanic reaction can also occur.

Generally, these multi-step strategies are the most commonly reported ones in the literature [42]. In the next sections, we review some of the most common wet-chemistry syntheses used to prepare Cu-based NWs.

2.3. Cu-Ni

The most promising bimetallic NW reported in the literature is the composite CuNi. The interest in combining Cu with Ni lies in three primary reasons: (1) high abundance of nickel on earth (2) relative miscibility of copper and nickel in the bulk state 3) high increase of stability due to non-corrosive properties of Ni. It should be noted that nickel is much less conductive than copper (1.43×10^7 S m^{-1} v^{-1}s^{-1}. 5.96×10^7 S m^{-1} [43]). This means that the Ni shell needs to be: (1) fabricated as thin as possible so as not to negatively impact the electrical properties of Cu, but also (2) thick enough for its oxidation-resistance capability to be retained. In bulk state, Cu and Ni form solid solutions with fcc structures at temperatures as low as 250 °C, depending on the composition [44]. They have similar atomic radii (size mismatch ~ 2%), the same crystal structures (fcc), same valence (+2), and similar electronegativity (~ 2% difference). However, their redox potentials are different ($E°(Ni^{2+}/Ni) = -0.23$ V; $E°(Cu^{2+}/Cu) = +0.34$ V) and a miscibility gap at low temperatures is notable, making the formation of a true alloy synthetically unviable as co-reduction isn't possible at lower temperatures. The alloy formation requires a substantial heat treatment (> ~250 °C). However, it should be noted that, at the nano scale, the temperature threshold for alloy formation is lowered, which is attributed to the high surface free energy of the Cu and Ni particles [26]. Ultimately, the most commonly reported CuNi NW systems exhibit a core@shell architecture with nickel at the surface. Most wet chemistry approaches are mainly based on reduction of the precursors in aqueous or alcoholic medium [45–62, 69] or via electrodeposition [63–68]. Typically, CuNi NWs can be synthesized either in a one-step process or in a two-step process. In a two-step process, Ni^{2+} ions are reduced onto the Cu template, while in a one step process, the Ni shell formation begins once the majority of Cu^{2+} ions are reduced, and the galvanic replacement isn't occurring anymore. However, in both one-step and two-step approaches, every mentioned step is riddled with variables such as: choice of the shaping agent, solvent, precursor, stabilizing agents, working temperatures, etc and changing them leads to different results.

Zhang *et al* [60] first reported a one-pot, one-step, synthesis of well-defined, smooth, core–shell Cu@Ni NWs in 2010. Ethylenediamine (EDA) was used as the shaping agent and hydrazine as the reductant in 7M NaOH. The synthesis yields NWs with diameters and lengths of NWs in the range of 200–300 nm and tens of micrometers, respectively. The alkaline media lowers the standard reduction potential of hydrazine to −1.23 V ($N_2H_4 + 4OH^- = N_2 + 4H_2O + 4e^-$), further enabling the use of relatively low temperatures for the precursor reduction (~80 °C) [56]. EDA, as well as other primary alkylamine-function shaping agents (notably, oleylamine (OAm)), have been shown to form a complex with Cu^{2+} ions, and to favor the anisotropic growth by selectively and strongly attach to the growing nanocrystals [70, 71]. Since this pioneering work, the use of hydrazine in alkaline media for Cu@Ni NWs has become a common approach in a one-pot, one-step, colloidal synthesis route [45, 46, 50, 56, 59, 60, 62]. The main drawback of the one-step EDA/hydrazine approach is that it typically results in NWs with a high average diameter, and it lacks an overall high level of control over the NW composition, as well as the dimensions, hence the need for a more nuanced two-step approach. Having that in mind, the same methodology can also be applied to a two-step synthesis approach by adding pre-made Cu NWs to an ethylene glycol–PVP system and using hydrazine to reduce the Ni precursor onto the Cu templates [45, 54]. Recently, Cu@Ni synthesis is most commonly reported to be conducted in 2 steps [45, 49–52, 54, 55, 59, 61] as separating core and shell formation allows for more controlled settings, leading to more homogeneous, monocrystalline, better defined core–shell structures.

The second notable colloidal chemical synthesis route is the oleylamine route. This approach relies on the use of OAm instead of EDA [45, 47–49, 51, 52, 55, 58, 61] in the absence of hydrazine. In this approach, OAm serves multiple roles: weak reductant, shaping agent, and stabilizer. Preparing the Cu@Ni NWs this way results in an advantage of the NWs being soluble in non-polar solvents, as they remain coated with OAm at the end of the synthesis. Since OAm is a weak reductant, higher temperatures are needed for the reduction of precursors to occur than in a typical hydrazine/EDA route - typically around 160 °C–190 °C for core@shell [45, 47–49, 51, 52, 55], and around 205 °C–230 °C for alloyed systems [49, 51, 52, 58]. The use of a weaker reductant serves an important purpose, as it allows the thermodynamically controlled synthesis to unfold rather than a mainly kinetically controlled one - which is the case with strong reductants. The first to introduce this approach was

Guo *et al* in 2013 [52]. When preparing the bimetallic NWs, in the first step, the reaction temperature is 180 °C which ensures the formation of pure Cu NWs. Ni^{2+} is considered to play a significant role in this step in the reduction of Cu through galvanic replacement [72–74]. In the second step, the temperature is increased to 210 °C to form the Ni shell. Additionally, the remnants of leftover Cu^{2+} are reduced into Cu on the Ni NW surface due to galvanic replacement, hence the alloy CuNi shell. The synthesis is highly selective, in the case of pure Cu NWs, 95% of the products are NWs, with a uniform diameter of 15 ± 2 nm. In the case of Cu@CuNi, an average diameter of 38 ± 4 nm containing up to 28 at% Ni can be produced. This level of shape and size control is highly superior to the hydrazine/EDA route. Precursor choice plays a major role in an OAm route synthesis. Notably, it was reported in multiple publications that the presence of chloride was shown to have a dramatic effect on the final shape of the nanoparticles [52, 75]. The Cl^- ions may act as a shaping agent, with a role similar to that of OAm. In regard to the shape of the NWs, generally, high Ni content (>20%) in the reaction medium yields a rough, corn-like structure of the Ni shell. However, the same synthesis can be used to produce a smooth shell surface just by changing the stirring speed, suggesting the impact of the kinetics on the shell formation. There are no reports on a typical OAm route synthesis being conducted in one step, presumably since, as discussed earlier, not separating the Cu core and Ni shell formation leads to the loss of control over the diameter and shape, a problem commonly associated with one-step syntheses for Cu@Ni NWs. A way to improve upon the primary alkylamine based route further would be to establish a way to do it in a water-based reaction medium. This is rather challenging, as OAm and similar alkylamines are typically not soluble in water. The report of Hazarika *et al* [48] shows one of the first syntheses which utilizes hexamethylenediamine (HDA), another primary alkylamine, instead of OAm in distilled water, with otherwise same characteristics of an OAm route, further extending it to the possibility of utilizing other primary alkylamines. This synthesis in this case was done in one step and yields Cu@Ni NWs with a lower aspect ratio, as well as in a less homogeneous diameter, ranging from ~125 to 185 nm. This result is probably due to the low solubility of HDA in water coupled with previously discussed problems related to a one-step synthesis. An interesting variation of a primary alkylamine synthesis route of Cu NWs was reported by Zhang *et al* [76], and this route includes the use of liquid molten crystals, formed by melted HDA and cetyltrimethylammonium bromide (CTAB) due to their amphiphilic nature. Based on this synthesis, the same route was taken by Wang *et al* [55] to produce Cu@Ni NWs with fairly uniform diameters and high aspect ratios.

One of the most commonly used strategies for preparing NWs in general is the 'polyol route', notably, most commonly used for the preparation of Ag NWs with a high level of control [77–79]. However, a reliable polyol synthesis applicable to Cu@Ni and Cu NWs in general is yet to be established. One of the notable probable reasons for this is that the reduction process of Cu^{2+} and Ni^{2+} requires the formation of intermediary oxidized species [53]. Moreover, reproducibility poses a major issue with the polyol process in general. As an answer to this, Ishijima *et al* [53] reported an alternative technique that utilizes mono-alcohols (most notably, 1-heptanol) instead of polyols as solvents and reductants, with OAm as the shaping agent. Wu *et al* [57] reported a similar approach, where benzyl alcohol was used instead. In general, this route is highly sensitive to the alcohol and metallic precursor salt choice, and ultimately suffers from problems characteristic for a polyol synthesis of anisotropic nanoparticles in one step—lack of control over the composition and dimension. Isotropic shapes are much easier to obtain and their processes of formation during a polyol synthesis are better controlled and understood [79].

Finally, one more route is commonly used for the preparation of Cu@Ni NWs electro and electroless plating. This deposition method was adopted because of its simplicity and high deposition rates. Chen *et al* [63] first reported on utilizing electrodeposition to prepare Cu@Ni core@shell nanowires. A pre-made Cu NW network was deposited on a glass substrate with Ni^{2+} in deaerated borate buffer (pH 9.2) at room temperature. The pre-made electrode containing deposited Cu NW templates was introduced into the plating bath for the deposition of Ni, with or without induced current. Ultimately, a very similar methodology is applied to other reports of preparing Cu@Ni core–shell NWs by electroless plating, with the Ni shell being amorphous or polycrystalline [63, 67].

2.4. Cu-Ag

Copper and silver are the most conductive metals, and especially in regard to TE applications, it's clear why producing CuAg bimetallic NWs is of great interest. However, attempts at alloying Cu and Ag are faced with a wide range of problems that make combining these elements into a true alloy highly unviable. Notably, standard redox potentials of Cu^{2+}/Cu and Ag^+/Ag are +0.34 V and +0.80 V, respectively. The fact that silver has a significantly higher redox potential deems co-reduction impossible and successive reduction very difficult, as it would require Ag^+ ions to be reduced onto metallic Ag on Cu NW surface to form Cu@Ag nanostructures. This generally leads to galvanic replacement, as Ag^+ ions are reduced to Ag atoms by oxidizing Cu atoms into Cu^{2+}, which results in cavitation or hollow structures. As explained above in section 2.2, this is a problem typically

occurring when trying to coat less noble metals with those that are more noble. The Kirkendall effect plays an additional role in altering the Cu/Ag interface. It leads to the outward diffusion of Cu atoms from the core to the surface of the Ag shell, leaving vacancies behind (Kirkendall voidening). Unlike in the case of Cu and Ni, Cu and Ag have a discrepancy in most parameters of importance for the preparation of alloyed nanoparticles (table 1). Ag has lower surface energy, and weaker cohesion with Cu due to its larger atomic size than copper. The lattice-mismatch strain between Ag and Cu is large (~12.6%) [80], leading to high structural unviability. All these factors favor the segregation of the two elements, with Ag going to the NW surface. This provides some insight into why all of the reported CuAg syntheses result in a core–shell architecture. To the best of our knowledge, there are no reports on true alloy CuAg NWs in the literature as of now. Having all of this in mind, it is clear that different strategies must be employed when attempting to prepare CuAg NWs, and that suppressing the galvanic replacement is the priority. The most recent synthesis approaches to achieve this are doing so through either lowering the redox potential of Ag through complexing with other compounds (most notably amines) [81–84], or by introducing another reductant to limit the galvanic replacement (commonly, ascorbic acid) [78, 85–87]. However, there is also an abundance of reports that exploit the naturally occurring galvanic replacement, with strategies designed to control it rather than suppress it (88–94). Virtually all of the syntheses in the literature are reported to be done in 2 steps: the preparation of Cu NWs, followed by that of the Ag shell. This is so for two main reasons: (1) interferences due to the differences in redox potentials and galvanic replacement, (2) mismatch in the reaction settings needed for Cu NWs and for the Ag coating. Namely, while most of the syntheses of Cu NWs are done through a hydrothermal route (glucose/HDA, Hydrazine/EDA), they're always done in the presence of a capping agent of the alkylamine type, deeming the prepared NWs not redispersible in water at the end of the synthesis. Contrary to that, an aqueous solution is necessary for coating with silver, hence the necessity of doing the synthesis in two steps. Han *et al* [81] were the first to report a Cu@Ag NW synthesis in 2012, and this synthesis was conducted in two steps. In the first step, Cu NWs were prepared by the OAm route. In the second step, $AgNO_3$ was introduced into the reactor along with dodecylamine (DDA) and left at 80 °C for 6 h. This reaction follows a simple trajectory—reduce the Ag precursor onto the pre-made Cu NWs, while relatively suppressing the galvanic replacement with DDA. However, due to all the problems discussed at the start of this section, heteroepitaxial growth of Ag on Cu NWs occurred in the form of 'islands' of separate nanocrystals rather than a uniform coating. In general, galvanic replacement based synthesis routes [81, 88–94] for Cu@Ag are simple and quick to conduct, but suffer from the following downsides: uneven Ag deposition, polycrystalline Ag, possible Kirkendall voidening, etching/roughening of the NW surface, hollowing of the NWs, etc. Various strategies have been reported to help control the galvanic replacement process. Sun *et al* [89] hypothesized that the surface roughness of Cu NWs plays an important role in the efficiency and uniformity of Ag shell deposition, with rough Cu NWs resulting in a more uniform Ag shell. The Ag/Cu precursor molar ratio is reported to be of great significance as well. Higher amounts of Ag lead to more prominent hollowing and etching, and the effect gets more prominent the longer the galvanic replacement reaction takes place [88, 89, 91–94]. Stewart *et al* [85] first reported the use of ascorbic acid for the prevention of Cu being affected by the galvanic replacement. By doing so, galvanic etching was avoided and Cu NWs were coated with a significantly more homogeneous Ag shell than when ascorbic acid wasn't present in the reaction medium. The roles of ascorbic acid in a Cu@Ag NW synthesis are twofold: (1) copper oxide is removed from the Cu NW surface, (2) it acts as an electron donor, actively reducing Cu oxidized species to metallic Cu that has appeared due to galvanic replacement. Due to these reasons, others report the use of the ascorbic acid-mediated Cu@Ag synthesis route resulting in a relatively uniform Ag shell [85, 87]. Another previously mentioned synthesis route for inhibiting galvanic replacement was first reported by Zhang *et al* In 2019 [82]: introducing the use of 2-ethylhexylamine. The synthesis is mediated by the formation of an Ag-amine complex ($[Ag(NH_2R)_2]^+$). This synthesis route follows the following trajectory: first, Cu NWs are prepared. Next, Ag-amine complex is introduced into a reaction medium containing the pre-made Cu NWs, and it covers the Cu NWs surface uniformly, resulting in a Cu@Ag-amine core–shell structure. Since the redox potential of this complex is relatively close to that of metallic copper, the galvanic replacement is completely bypassed. Finally, the complex is decomposed by an annealing process in air (140 °C for 5 min), resulting in Cu@Ag core–shell NWs with a rough, but uniform report Ag shell. Another report describes the use of 2-ethylhexylamine for the same purpose [84], while Rahul *et al* [83] utilized 3-Dimethylamino-1,2 propanediol, both resulting in a rough but uniform Ag shell.

2.5. Cu-Au

Combining copper and gold shares the bulk of the phenomena associated with the Cu@Ag system. Notably, the persisting problem regarding the deposition of a more noble metal onto a less noble one, resulted in galvanic replacement and the Kirkendall effect. However, when compared to the CuAg system, CuAu exhibits higher miscibility, making the combination of two elements into a real alloy or otherwise easier than in the case of Cu and Ag due to higher compatibility concerning the crystal lattices. Au and Cu are completely soluble at

temperatures higher than 410 °C, while they exhibit partial miscibility at temperatures as low as ~200 °C. In case of lower temperatures, the formation of the intermetallic phases Au_3Cu, AuCu (tetragonal or orthorhombic), and $AuCu_3$ can occur [95, 96]. That being said, a frequent necessity for preparing CuAu NWs is thermal annealing, commonly reported for alloyed CuAu systems in the literature, for nano-objects or otherwise. The first report of coating Cu NWs with a Au shell stems from the work of Stewart *et al* [85], and that same synthesis, previously discussed in the CuAg section, was utilized. The synthesis is mediated by galvanic replacement for the reduction of Au. Ascorbic acid was utilized to protect the Cu NWs from galvanic etching and hollowing, and it resulted in a homogeneous Au coating on the Cu NWs. In the same work, it was shown how, considering that Cu NWs aren't highly oxidized to begin with, coating the NWs with a more noble metal resulted in the hollowing of the NWs, ultimately presenting nanotubes as the final product. This presents a good example of how, without an appropriate strategy to prevent galvanic replacement from happening, obtaining a bimetallic nanostructure isn't viable. Following this work, different strategies are presented to obtain CuAu NWs. In the work of Niu *et al* [97], several strategies were explored—(1) injecting $HAuCl_4$ dispersed in OAm rapidly into the reactor containing Cu NWs at an operating temperature of 140 °C, (2) doing the same, but slowly feeding $HAuCl_4$ into the growth solution via syringe pump, and (3) utilizing trioctylphosphine (TOP) to replace OAm in dissolving the gold precursor and form a complex with Au, resulting in a lower redox potential and hence protecting the Cu NWs from galvanic etching. The first route resulted in small Au NPs instead of an Au shell due to instantaneous reduction leading to homogeneous nucleation. The second route led to a high degree of etching on Cu NWs due to galvanic replacement. Finally, the third route resulted in a uniform Au shell on top of Cu NWs with an average diameter of 21 ± 4 nm, without any observed surface damage. In 2020, Niu *et al* [23] utilized the just described approach [97] and further thermally annealed the Cu@Au NWs to transform them into fully ordered Cu_3Au NWs. To be able to achieve this, shape preservation during the thermal treatment is key, and to do that, Niu *et al* turned to preparing Cu NWs with a high level of defects that can further facilitate disorder-to-order transition at lower annealing temperatures [98, 99]. The prepared Cu@Au NWs were deposited onto glass slides, and were annealed in a hydrogen/argon mixture. Once the annealing temperature reached 200 °C the bulk of the Au atoms were no longer restricted on the surface of Cu NWs, but spread inward into the NW core, and this trend continued to be observed as the temperature increased. Finally, at 320 °C, the final NW composition was achieved - Cu_3Au NWs, wherein the Cu and Au atoms were homogeneously distributed. Another strategy to tackle heterogeneous deposition of the Au shell and to prevent etching of Cu NWs was reported by Kim *et al* [100]. The first aspect of the reported route is based on providing an alternative electron provider to prevent Cu from oxidizing on behalf of Au reduction, and for this purpose, diethylhydroxylamine (DEHA) was used. Secondly, to ensure homogeneous distribution, ligand exchange was conducted, substituting the pre-existing HDA on the Cu NW surface with PVP. The reason for this lies in the fact that PVP oxygen atoms bind with the surface of the Cu NWs more strongly than HAD amine group does. Zhang *et al* [101] resorted to electroplating instead of a colloidal synthesis. In this work, pre-made Cu NWs were deposited onto a polyethylene terephthalate (PET) substrate, and they were subsequently coated through a two-electrode electrodeposition process, with $KAu(CN)_2$ $KAg(CN)_2$ used as precursors. This way, a Cu core and AgAu alloy shell NW network was prepared, however, the same protocol can be used for the preparation of Cu@Au core–shell network as well. Ultimately, utilizing current and turning to electroplating instead of colloidal synthesis helps with bypassing the galvanic replacement-related problems, which were already discussed in depth. Zhang *et al* [102] showcase the use of electrodeposition as well, and experimenting with different sets of parameters was done with the goal to combine and control the effect of electrochemical and galvanic displacement reactions, ultimately resulting in an alloyed CuAu NW network.

2.6. Cu-Sn

Unlike previously discussed noble metals, tin is much more compatible with copper in many regards. Firstly, Cu and Sn exhibit rather high miscibility, ensuring that they can be combined in a true alloy in many different ratios [103]. Secondly, the redox potentials of Sn and Cu (-0.14 V and $+0.34$ V, respectively) make working with these two metals easier as galvanic replacement doesn't occur. However, the low redox potential of Sn can present as a drawback, as it can lead to quick oxidation and formation of SnO_2, as $Sn^{+4/+2}$ are the most stable oxidation states of tin, rather than Sn^0. Concerning NW synthesis, it leads to the formation of SnO_2 nanoparticles which can be difficult to control. In the study of Ye *et al* [59], the electroplating route was explored for coating Cu with various other metals, Sn being among them. In this case, constant-potential electroplating at -0.65 V wasn't a viable option for coating pre-made Cu NWs with tin, as it resulted in uneven coatings consisting of nanoparticles, and hence, cyclic voltammetry scans were utilized instead. Electrodeposition is a commonly reported route for coating Cu NWs with a Sn shell [104–107]. Chen *et al* [106] reported first growing Cu NWs from Cu foam, and subsequently electroplating Sn on top of Cu NWs by applying a constant current density, resulting in Cu NWs coated with well-distributed Sn nanoparticles, rather than a uniform coating. Li *et al* [105]

reported a similar methodology: by mixing a commercial plating solution of Cu and Sn and reducing them simultaneously, mixed alloyed NWs of the following atomic percentages with Cu considered as 100%: Sn–8% , Sn–43% and Sn–86% were prepared. Lai *et al* [107] reported the preparation of core–shell Cu@SnO_2 NWs by first utilizing template-directed electrodeposition of SnO_2 nanotubes, which was followed by subsequent electrodeposition of a metallic copper core within SnO_2 nanotubes. Another approach for coating Cu NWs with Sn is sputtering, as demonstrated by Wang *et al* [108] where 99.99% pure Tin was sputtered on a pre-prepared Cu NW array at a working pressure of 10 Pa, resulting in a CuSn alloyed NWs. Alloyed CuSn NWs can also be prepared by thermally annealing Cu@Sn core–shell NWs, as demonstrated by Hu *et al* [109]. To the best of our knowledge, only one report of preparation of CuSn NWs by colloidal synthesis exists up to this date, a report by Wang *et al* [110]. In this report, a one-step, one-pot synthesis was presented. OAm was used as a shaping agent and a soft reductant, glucose as the primary reductant, and along with the metallic precursor, the reaction mixture was heated at 120 °C for about 12 h in a Teflon® sealed autoclave, which yielded in Cu@Sn core–shell NWs with an amorphous Sn species as the shell. Furthermore, annealing the prepared Cu@Sn NWs resulted in the formation of alloyed NWs.

2.7. Cu-Zn

Combining Cu with Zn shares many similarities with the previously discussed Cu-Sn system. Firstly, as with Sn, the low redox potential of Zn ensures that galvanic etching of Cu NWs doesn't occur when Zn is coated onto it. However, the low redox potential also results in metallic Zn readily oxidizing to Zn^{2+}, resulting in the formation of ZnO. This however is not necessarily always a downside, because just like SnO_2, ZnO is highly transparent - which is particularly useful for TE preparation. To avoid ZnO formation however, Cu and Zn must form an alloy. In fact, Cu and Zn are widely known to be combined into an alloy—most famously, that alloy being brass. This is attributed to relatively high miscibility rates even in lower temperatures (maximum solubility of Zn in Cu (38% at 456 °C) and solubility of Zn in Cu at room temperature (30% at 20 °C) [111]. Henceforth, regarding Cu-Zn NWs, preparation of alloyed species is commonly reported [112–116], but Cu@Zn and Cu@ZnO_2 core–shell NWs are reported as well [55, 113, 117–119] as the high transparency of ZnO is a positive property, especially in regard to TE applications. While the first report on coating electrospun Cu NWs with Zn was conducted with the use of atomic layer deposition [119], the most commonly reported way of obtaining Cu-Zn NWs is by far by electrodeposition [60, 112–117]. Typically, the electrodeposition was followed by thermal annealing, with temperatures varying in dependence of the intended final product (alloy, Cu@ZnO, etc.). There are two reports of preparation of Cu-Zn NWs by electrodeposition in ionic liquids (ILs) [113, 115], which is a class of salts that are in liquid state at temperatures below 100 °C, differentiating them from high-temperature molten salts. The main benefits of utilizing ILs for the preparation of ordered metallic deposits when compared to aqueous solutions and the conventional organic solvents are the wide electrochemical window, high thermal stability, negligible vapor pressure, low flammability, and intrinsic ionic conductivity [115]. Additionally, utilizing ILs has 2 benefits: (1) the higher available operating temperature of ILs favors the formation of deposits with good crystallinity; (2) since ILs are aprotic, the problems associated with hydrogen evolution during electrodeposition are eliminated. To the best of our knowledge, only one report of Cu-Zn NWs preparation by colloidal synthesis can be found in the literature, reported by Wang *et al* [55]. The synthesis reported is a one-pot, two-step, OAm mediated synthesis, resulting in core–shell Cu@Zn NWs.

3. Fabrication of the NW network and the post-treatments

Transparent conducting films can be made from bimetallic NWs using a number of different cost-effective and up-scalable coating methods, unlike the traditional methods associated with the preparation of TCO (figure 2 right panel).

Namely, sputtering is the most common method to prepare TCOs, which requires a vacuum chamber, as well as high temperature. On the other hand, the most commonly used fabrication methods for preparation of MNW based TEs require neither. The most commonly used methods for MNW deposition fall into the coating methods categories, so: drop casting, spray-coating, Mayer-rod coating, spin-coating. Spray-coating is by far the most reported deposition method [120–128]. The reason why this method is highly reported stems from the following factors: it is easy to set up and use, quick, reproducible, and the parameters are easily modified to fit the needs of the targeted TE. This way, NW networks of different densities can be produced, leading to a wide variety of possibilities in regard to transparency and conductivity of the deposited NW network. Another advantage of these spray-coating approaches is the industrial upscaling. They are suitable for the deposition of (bi-)metallic NWs on large-sized substrates.

Nanowire networks have to be further processed after coating to improve the conductivity of the films. Many of the studies discussed in this review report large initial resistance in the as-deposited NW films. The reason for

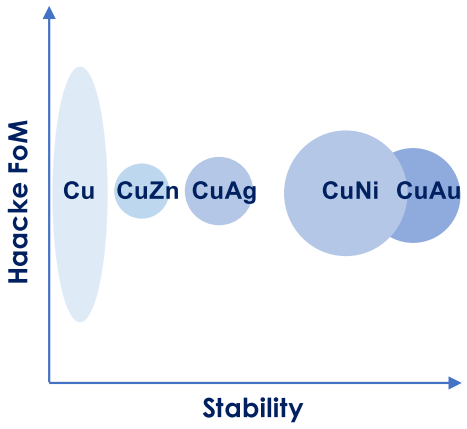

Nanowire	T(%) (550 nm)	R (Ω sq^{-1})	Ageing conditions	Stability (days)	Ref.
CuZn	82	30	air	17	[115]
CuAg					
	80	30	High T/ humidity	At least 30	[82]
	89	13	High T/ humidity	At least 20	[83]
CuNi					
	85	30	air	30	[51]
	93	66	air	100	[55]
	84	30	air	30	[58]
CuAu	90	14	air	40	[97]
	87	23	acidic env.	7	[103]

Figure 3. Comparison of TEs fabricated with different Cu-based nanowires. This figure shows the general trend with two criteria: stability and Haacke's figure of merit. The Haacke's figure of merit links the optical and electrical properties [3]. Since the material selection is condition-dependent, the marks are only general indications. The size of the circle is proportional to the amount of data. Note that there are no reports of stability studies for CuSnNW networks. Summary of optical transmittance (T), sheet resistance (R) and stability for various types of bimetallic nanowires, data extracted from some recent references.

this lies in NW-NW junction resistance, which is intrinsically high for a variety of reasons. Firstly, when MNWs are deposited onto the substrate (electroplating not included in this aspect), they lack efficient contact between each other. One of the reasons for this is the presence of residual organic residues from the synthesis and/or the formation of the surface oxide which must be eliminated.

Another critical reason for high junction resistance, which is present in all MNW networks, but especially relevant for copper-based bimetallic core–shell NWs is the fact that the main conduit for current transfer lies in the Cu core. Due to the presence of another metal in the form of a shell, the superimposed NWs lack Cu-Cu contact, since the bimetallic NWs are simply physically overlapping. As an example, in the case of Cu@Ni core–shell NWs, the main species present in the NW-NW contact regions is Ni/oxidized Ni form, which is much less conductive than Cu. This phenomenon has less of an impact on the NW network in the case of the Cu@Ag NWs as Ag already has intrinsically high conductivity, but even in this case, optimal conductivity can only be reached if the NWs were fused together, ensuring a more efficient contact in the junctions. To do so, as well as to rid the NWs of the remnant organic residue, post treatments must be conducted following the deposition of the MNW network. Various approaches have been reported for post treatments on deposited MNW networks, but the most broadly utilized ones are: (1) thermal annealing [45, 51, 54, 55, 58, 67, 82, 97, 114, 117], (2) plasma treatments [51, 54, 117], (3) acid mediated treatments [64, 67, 68], (4) utilizing mechanical pressure to fuse the NWs [46, 68], or (5) light irradiation sintering [129, 130]. These post treatments result in a drastic decrease of the MNW network resistivity, usually from 10^4 or 10^5 Ω sq^{-1} to about a few or few tens of Ω sq^{-1}. Thermal annealing is typically conducted in simple settings, oftentimes in an oven/furnace, in temperatures ranging from 175 °C–220 °C, and the duration of the treatments being as short as 5 min [82], but in most cases ranging from 30 min to 1 h [45, 51, 55, 58, 67, 68, 97, 114, 117]. Plasma treatments are usually shorter, and most commonly they are conducted in an atmosphere of 95% nitrogen and 5% hydrogen. Mechanical pressure-mediated post treatments are even shorter, lasting typically 1 min or so, with the mechanical pressure applied to the NW network in the scale of ~8 MPa. Light-induced plasmonic nano-welding reduces network resistance thanks to efficient localized heating compatible with flexible substrates [129, 130]. While all of the aforementioned post treatments are effective, sustainability and restriction of the use of energy should always be a priority, hence, post treatments that don't rely on the aforementioned are favorable in that regard. Acid based treatments are one example of such treatments, as well as acetone/water rinsing [85], and the H_2O_2 treatment [84], however—they are less effective and require multiple repeats. Another aspect that must be considered in regard to post-treatments is substrate choice, as certain post-treatments have a detrimental impact on substrates. As an example, thermal annealing cannot be conducted on a MNW network deposited on PET and if it was to be conducted, it must be done on a glass substrate. Consequentially, MNW network preparation methods that rely on thermal annealing yield in non-flexible TEs. Finally, one way to bypass the need for the post treatments altogether is to prepare the MNW by electrodeposition, as it typically results in the fusion of the NWs during the preparation [37, 63, 65, 66, 101, 114, 117]. However, the efficiency of the NW fusion during the electrodeposition is not always sufficient, and multiple studies report the necessity of utilizing one of the

aforementioned post treatment methods on the NW network prior to depositing the second metal onto the first one [64, 114, 117].

Producing bimetallic nanowires drastically improves the long-term stability of Cu-based TEs in devices. Figure 3 provides a general summary of the current situation related to the above bimetallic nanostructures, showing their main key features: the long-term stability and the Haacke's figure of merit (FoM) which evaluates two main and most important aspects of electrodes, i.e. optical transparency and electrical conductivity. The figure compares the performance of TEs fabricated with monometallic and bimetallic nanowires. While almost good electrical and optical properties can be achieved both with monometallic and bimetallic nanostructures, the stability of the bimetallic NWs is much higher. To date, the most efficient approach toward enhanced copper NW stability is to coat or alloy it with gold. Such coupling clearly delays network degradation. Thus, the above systems can solve some of the inherent shortcomings of Cu NWs and environmental sensitivity.

4. Conclusions and perspectives

Metallic TEs have become a mature technology that can now exhibit promising properties and address efficiently many fields of application. MNWs offer high transparency and low levels of electrical resistance, combined with excellent bendability and good stretchability. The main investigated are Ag NW and Cu NW. As the abundance of Ag is very similar to that of In, Cu NW networks represent the most promising alternative for the future. However, Cu NW networks suffer from high instability in air, and this problem must be addressed if Cu NW networks are to be a serious candidate for next-generation TEs. One of the ways to mitigate the instability-related problems is by producing bimetallic NWs.

Preparing bimetallic NPs however presents a challenge due to the fact that a wide range of parameters of the two metals must be aligned for the synthesis to be successful. Moreover, inducing the growth of uniform anisotropic architectures requires a high level of control over the system which remains very difficult to achieve. Nevertheless, there are many extensive studies reporting the preparation of CuM NWs and the means to prepare them, with the most commonly reported systems being: CuNi, CuAg, CuAu, CuSn, and CuZn (table 2). It should be noted that coating Cu NWs with more noble metals proves to be very difficult as it results in galvanic replacement. Other notable difficulties are those of rapid oxidation of Sn and Zn, applicable to Cu-Sn and Cu-Zn systems, leading to uneven deposition of oxide NPs and ultimately more brittle materials. The two most extensively reported strategies for the synthesis of CuM NWs are (1) colloidal synthesis, and (2) electroplating. Sometimes, the combination of both is used as well. The strategies reported vary and are done in either one or two steps, but typically, the reported routes follow a similar set of rules, most of which can be applied both to colloidal synthesis and electroplating:

- The presence of a shaping agent (HDA, OAm, EDA, etc.) is necessary for the unidirectional growth, leading to high aspect ratios needed for TEs
- Working temperatures ranging from ~100 °C to ~300 °C are utilized (higher T are associated with alloy formation) in colloidal synthesis, while in electroplating, when conducted in water or conventional organic solvent, tends to be much lower
- In colloidal synthesis, reductant choice can heavily impact the kinetics and should be chosen accordingly depending on the binary system of interest (soft reductants (glucose) versus strong reductants (hydrazine))
- Stabilizing components & complexing agents (typically used for the modification of the redox potential) are sometimes necessary, both in colloidal synthesis and in electroplating
- Choice of the precursor metal salts can be highly important for the final product (e.g. positive impact of Cl^- ions on unidirectional growth) (applicable for all of the routes)

As for the yet unexplored Cu based NWs, one of the promising such systems for further prospects is to consider the fabrication of alloys containing several metals. The metallurgy of bulk alloys has advanced dramatically in the last decade with the introduction of non-conventional alloys such as the stable high entropy alloy. We can foresee the same trend will happen in nanoalloys of aspect ratio. The fabrication of nanowires containing several metals will produce new properties and possibly a higher degree of fabrication control. Another obvious path for advancing in this field of targeted applications is to consider the development of nanocomposite systems. For instance, Cu-core F-doped SnO_2-shell NWs could significantly impact both the conductivity and the stability of Cu NWs in a positive manner.

It is important to emphasize the problems with the intrinsic conductivity of the MNW networks. High initial resistivity of the deposited MNW networks stemming from poor efficiency of the NW-NW contact and the

residual organic residue necessitates the utilization of post treatments upon deposition; the most commonly reported ones being thermal annealing, application of mechanical pressure, plasma cleaning treatments, and acid-based treatments. Again, sustainability must be a priority when utilizing treatments that require high-energy consumption, as if MNW networks were to be used in commercial settings, the energy output needs to be decreased as much as possible. Acid-based treatments represent one such most interesting alternative.

Ultimately, synthesis of bimetallic NWs is rather complex, and more work is needed to gain better control over the architecture, composition, and uniformity of the Cu-M NWs. Computational chemistry might prove to be the leading factor in the current state of the art in the field of nanoalloys, as by uncovering the mechanism intricacies of how these species are formed, we gain more insight on how to control them [131]. Furthermore, with the advances in artificial intelligence and machine learning techniques, time spent modeling these structures could be of worth, especially as the structures become more complex [132, 133]. We have now the instrumentation, analytical and theoretical methods needed for the advancement of this field.

Acknowledgments

This work was supported by the French National Research Agency (ANR) under the reference *ANR-18-CE09–0040–03* (MEANING project) and Solvay S.A.

Data availability statement

No new data were created or analysed in this study.

Conflicts of interest

The authors declare no conflicts of interest.

ORCID iDs

Anđela Križan https://orcid.org/0009-0009-2111-8570
Emmanuel Opeyemi Idowu https://orcid.org/0000-0001-7358-7314
Etienne Duguet https://orcid.org/0000-0002-0675-5987
Mona Tréguer-Delapierre https://orcid.org/0000-0002-3096-6645

References

[1] Lu X, Zhang Y and Zheng Z 2021 *Adv. Electron. Mater.* **7** 2001121
[2] Lu H, Ren X, Ouyang D and Choy W C 2018 *Small* **14** 1703140
[3] Papanastasiou D T, Schultheiss A, Muñoz-Rojas D, Celle C, Carella A, Simonato J P and Bellet D 2020 *Adv. Funct. Mater.* **30** 1
[4] Liu C, Xiao C, Xie C and Li W 2021 *Nano Energy* **89** 106399
[5] Dataintelo 2022 *Transparent Electrode Market Report, Available at:* https://dataintelo.com/report/transparent-electrode-market/ (accessed: 6 June 2023)
[6] Trading Economics 2023 Indium , Available at: https://tradingeconomics.com/commodity/indium (accessed: 12 July 2023)
[7] Girtan M and Negulescu B 2022 *Opt. Mater.* **13** 100122
[8] Ye S, Rathmell A R, Chen Z, Stewart I E and Wiley B J 2014 *Adv. Mater.* **26** 6670
[9] Nguyen V H, Papanastasiou D T, Resende J, Bardet L, Sannicolo T, Jiménez C, Muñoz-Rojas D, Nguyen N D and Bellet D 2022 *Small* **18** 2106006
[10] Chuang S, Gao Q, Kapadia R, Ford A C, Guo J and Javey A 2013 *Nano Lett.* **13** 555
[11] Celle C, Mayousse C, Moreau E, Basti H, Carella A and Simonato J-P 2012 *Nano Res.* **5** 427
[12] Zhang Y, Kim M, Wang L, Verlinden P and Hallam B 2021 *Energy Environ. Sci.* **14** 5587–610
[13] Hallam B, Kim M, Zhang Y, Wang L, Lennon A, Verlinden P, Altermatt P P and Dias P R 2022 *Prog. Photovolt.: Res.* **31** 598
[14] Daily Metal Price 2023 Daily Metal Price: Metal Price Tables and Charts, Available at https://dailymetalprice.com/ (accessed: 12 july 2023)
[15] Li Z, Chang S, Khuje S and Ren S 2021 *ACS Nano* **2021** 6211
[16] Li X, Wang Y, Yin C and Yin Z 2020 *J. Mater. Chem.* C **8** 849
[17] Wang Y and Yin Z 2019 *Appl. Sci. Converg. Technol.* **28** 186
[18] Patil J J, Woo R C, Trebach A, Carter K-J B, Wai E, Sannicolo T and Grossman J C 2021 *Adv. Mater.* **33** 2004356
[19] Xu L, Yang Y, Hu Z-W and Yu S-H 2016 *ACS Nano* **10** 3823
[20] Lu H, Wang R, Bao F, Ye J, Lin H, Zhu H, Wan M, Yang H, Shen K and Mai Y 2022 *Opt. Mat.* **133** 112848
[21] Han J, Sung C, Chi-Woo S, Kim Y and Kim T-Y 2023 *Sol. Energy Mater. Sol. Cells* **249** 112035
[22] Sharma G, Kumar A, Sharma S, Naushad M, Prakash Dwivedi R, ALOthman Z A and Mola G T 2019 *J. King Saud Univ. Sci.* **31** 257
[23] Niu Z, Chen S, Yu Y, Lei T, Dehestani A, Schierle-Arndt K and Yang P 2020 *Nano Res.* **13** 2564
[24] Davis J R 2008 *Copper and Copper Alloys* (ASM International) 4

[25] Lehr A, Jesús Velázquez-Salazar J, Montejano-Carrizales J M, Mejía-Rosales S, Rubén M-C, Bazan-Diaz L and Miguel Jose Y 2023 *Faraday Discuss.* **242** 10
[26] Ferrando R, Jellinek J and Johnston R L 2008 *Chem. Rev.* **108** 845
[27] Dean J W, Cowan M, Estes J, Ramadan M and Mpourmpakis G 2020 *ACS Nano* **14** 8171
[28] Eom N, Messing M E, Johansson J and Deppert K 2021 *ACS Nano* **15** 8883
[29] Ghosh A, Datta S and Dasgupta T S 2022 *J. Phys. Chem.* C **126** 6847
[30] Vitos L, Ruban A, Skriver H and Kollár J 1998 *Surf. Sci.* **411** 186
[31] Pauling L 1960 *The Nature of the Chemical Bond* 3rd edn (Cornell University Press) p 93
[32] Speight J G and Norbert A L 2017 *Lange's Handbook of Chemistry* 329
[33] Slater J C 1964 *J. Chem. Phys.* **41** 3199
[34] Xiao S, Hu W, Luo W, Wu Y, Li X and Deng H 2006 *Eur. Phys. J.* B **54** 479
[35] Bhanushali S, Ghosh P, Ganesh A and Cheng W 2015 *Small* **11** 1232
[36] Mott D, Galkowski J, Wang L, Luo J and Zhong C-J 2007 *Langmuir* **23** 5740
[37] Toimil-Molares M E 2012 *Beilstein J. Nanotechnol.* **3** 860
[38] Mohanty U S 2011 *J. Appl. Electrochem.* **41** 257
[39] Anderson B D and Tracy J B 2014 *Nanoscale* **6** 12195
[40] Liu X and Astruc D 2017 *Adv. Mater.* **29** 1605305
[41] Fan H J, Gösele U and Zacharias M 2007 *Small* **3** 1660
[42] Loza K, Heggen M and Epple M 2020 *Adv. Funct. Mater.* **30** 1909260
[43] Raymond A. Serway 1998 *Principles of Physics* 2nd edn (Saunders College Pub) p 602
[44] Okamoto H, Schlesinger M E and Mueller E M 2016 *Alloy Phase Diagrams* (Asm International)
[45] Rezaga B F Y and Balela M D L 2020 *Mater. Today Proc.* **22** 241
[46] Chen J, Chen J, Li Y, Zhou W, Feng X, Huang Q, Zheng J-G, Liu R, Ma Y and Huang W 2015 *Nanoscale* **7** 16874
[47] Guo H, Jin J, Chen Y, Liu X, Zeng D, Wang L and Peng D-L 2016 *Chem. Commun.* **52** 6918
[48] Hazarika A, Deka B K, Kim D, Jeong H E, Park Y-B and Park H W 2018 *Nano Lett.* **18** 6731
[49] Wu D, Zhang W and Cheng D 2017 *ACS Appl. Mater. Interfaces* **9** 19843
[50] Su C, Zhang L, Han Y, Ren C, Zeng M, Zhou Z, Su Y, Hu N, Wei H and Yang Z 2020 *Sens. Actuators B Chem.* **304** 127347
[51] Wang X, Wang R, Shi L and Sun J 2015 *Small* **11** 4737
[52] Guo H, Chen Y, Ping H, Jin J and Peng D-L 2013 *Nanoscale* **5** 2394
[53] Ishijima M, Huaman J L C, Yokoyama S, Shinoda K, Uchikoshi M, Miyamura H and Jeyadevan B 2018 *New J. Chem.* **42** 13044
[54] Rathmell A R, Nguyen M, Chi M and Wiley B J 2012 *Nano Lett.* **12** 3193
[55] Wang H *et al* 2016 *ACS Appl. Mater. Interfaces* **8** 28709
[56] Wang X, Dong L, Zhang B, Yu M and Liu J 2016 *Nanotechnology* **27** 125602
[57] Wu D, Tan Q and Hu L 2018 *Mater. Chem. Phys.* **206** 150
[58] Xue J, Song J, Zou Y, Huo C, Dong Y, Xu L, Li J and Zeng H 2016 *RSC Adv.* **6** 91394
[59] Ye S, Stewart I E, Chen Z, Li B, Rathmell A R and Wiley B J 2016 *Acc. Chem. Res.* **49** 442
[60] Zhang S and Zeng H C 2010 *Chem. Mater.* **22** 1282
[61] Liu Z, Xia G Q, Zhu F, Kim S, Markovic N, Chien C L and Searson P C 2008 *J. Appl. Phys.* **103** 6
[62] Udayabhaskar R, Ollakkan M S and Karthikeyan B 2014 *Appl. Phys. Lett.* **104** 013107
[63] Chen Z, Rathmell A R, Ye S, Wilson A R and Wiley B J 2013 *Angew. Chem. Int. Ed.* **52** 13708
[64] Zhang H, Wang S, Tian Y, Liu Y, Wen J, Huang Y, Hang C, Zheng Z and Wang C 2020 *Chem. Eng. J.* **390** 124495
[65] Yoshikawa R, Tenjimbayashi M, Matsubayashi T, Manabe K, Magagnin L, Monnai Y and Shiratori S 2018 *ACS Appl. Nano Mater.* **1** 860
[66] Duong T-H, Hoang H-M and Kim H-C 2019 *Chem. Eng. Commun.* **207** 652
[67] Kim K, Kwon H-C, Ma S, Lee E, Yun S-C, Jang G, Yang H and Moon J 2018 *ACS Appl. Mater. Interfaces* **10** 30337
[68] Stewart I E, Rathmell A R, Yan L, Ye S, Flowers P F, You W and Wiley B J 2014 *Nanoscale* **6** 5980
[69] Orgen S B and Balela M D L 2018 *Key Eng. Mater.* **775** 132
[70] Myung K K, Flowers P F, Stewart I, Ye S, Baek S, Jae N K and Wiley B J 2016 *J. Am. Chem. Soc.* **139** 277
[71] Jin M, He G, Zhang H, Zeng J, Xie Z and Xia Y 2011 *Angew. Chem. Int. Ed.* **50** 10560
[72] Zhang H, Jin M, Wang J, Li W, Camargo P H C, Kim M J, Yang D, Xie Z and Xia Y 2011 *J. Am. Chem. Soc.* **133** 6078
[73] Sun Y, Mayers B T and Xia Y 2002 *Nano Lett.* **2** 481
[74] Zhang W, Yang J and Lu X 2012 *ACS Nano* **6** 7397
[75] Guo H *et al* 2013 *Sci Rep.* **3** 1
[76] Zhang D, Wang R, Wen M, Weng D, Cui X, Sun J, Li H and Lu Y ,J 2012 *Am. Chem. Soc.* **134** 14283
[77] Sun Y, Gates B, Mayers B and Xia Y 2002 *Nano Lett.* **2** 165
[78] Sun Y and Xia Y 2002 *Adv. Mater.* **14** 833
[79] Fiévet F, Ammar-Merah S, Brayner R, Chau F, Giraud M, Mammeri F, Peron J, Piquemal J-Y, Sicard L and Viau G 2018 *Chem. Soc. Rev.* **47** 5187
[80] Tsvetanka Z, Jagannadham K and Narayan 1994 *J. Appl. Phys.* **75** 860
[81] Han M, Liu S, Zhang L, Zhang C, Tu W, Dai Z and Bao J 2012 *ACS Appl. Mater. Interfaces* **4** 6654
[82] Zhang B, Li W, Jiu J, Yang Y, Jing J, Suganuma K and Li C-F 2019 *Inorg. Chem.* **58** 3374
[83] Navik R, Ding X, Huijun T and Zhao Y 2020 *Ind. Eng. Chem.* **60** 263
[84] Zhang B, Li W, Nogi M, Chen C, Yang Y, Sugahara T, Koga H and Suganuma K 2019 *ACS Appl. Mater. Interfaces* **11** 18540
[85] Stewart I E, Ye S, Chen Z, Flowers P F and Wiley B J 2015 *Chem. Mater.* **27** 7788
[86] Catenacci M J, Reyes C, Cruz M A and Wiley B J 2018 *ACS Nano* **12** 3689
[87] Cruz M A, Ye S, Kim M J, Reyes C, Yang F, Flowers P F and Wiley B J 2018 *Part. Part. Syst. Charact.* **35** 1700385
[88] Wei Y, Chen S, Lin Y, Yang Z and Liu L 2015 *J. Mater. Chem.* C **3** 9594
[89] Sun Y, Zhang F, Xu L, Yin Z and Song X *2014, J. Mater. Chem.* A **2** 18583
[90] Weng W-L, Hsu C-Y, Lee J-S, Fan H-H and Liao C-N 2018 *Nanoscale* **10** 9862
[91] Meng X, Zhao S, Zhang Z, Zhang R, Li J, Leng J, Cao D, Zhang G and Sun R 2019 *J. Mater. Chem.* C **7** 7061
[92] Zhao J, Zhang D and Zhang X 2015 *Surf. Interface Anal.* **47** 529
[93] He X, He R, Lan Q, Duan F, Xiao J, Song M, Zhang M, Chen Y and Li Y 2016 *J. Nanomater.* **2016** 1
[94] Jiang Z, Tian Y, Ding S, Wen J and Wang C 2016 *CrystEngComm* **18** 1200

[95] Okamoto H, Chakrabarti D J, Laughlin D E and Massalski T B 1987 *J. Ph. Equilibria* **8** 454
[96] Meischein M, Meischein M, Hammerschmidt T, Xiao B, Zhang S, Lamya A, Scheu C and Ludwig A 2022 *Nanoscale Adv.* **4** 3855
[97] Niu Z *et al* 2017 *J. Am. Chem. Soc.* **139** 7348
[98] Yan Y C, Du J S, Gilroy K D, Yang D R, Xia Y N and Zhang H 2017 *Adv. Mater.* **29** 1605997
[99] Li J R and Sun S H 2019 *Acc. Chem. Res.* **52** 2015
[100] Kim D *et al* 2020 *Adv. Mater. Technol.* **5** 2000661
[101] Zhang H, Tian Y, Wang S, Huang Y, Wen J, Hang C, Zheng Z and Wang C 2020 *J. Chem. Eng.* **399** 125075
[102] Zhang H, Tian Y, Wang S, Feng J, Hang C, Wang C, Ma J, Hu X, Zheng Z and Dong H 2021 *J. Chem. Eng.* **426** 131438
[103] Karthik M, Abhinav J and Karthik V S 2021 *Met. Mater. Int.* **27** 1915
[104] Yin Q, Gao F, Gu Z, Stach E A and Zhou G 2015 *Nanoscale* **7** 4984
[105] Li X, Gu Z, Cho J, Sun H and Kurup P 2011 *Sens. Actuators B Chem.* **158** 199
[106] Chen G, Ye D, Chen R, Li J, Zhu X and Liao Q 2021 *J. CO2 Util.* **44** 101409
[107] Lai M, Mubeen S, Chartuprayoon N, Mulchandani A, Deshusses M A and Myung N V 2010 *Nanotechnology* **21** 295601
[108] Wang J, Du N, Zhang H, Yu J and Yang D 2011 *J. Phys. Chem. C* **115** 23620
[109] Hu H, Wang Y, Du N, Sun Y, Tang Y, Hu Q, Wan P, Dai L, Fisher A C and Yang X J 2018 *ChemElectroChem* **5** 3854
[110] Wang J, Ji Y, Shao Q, Yin R, Guo J, Li Y and Huang X 2019 *Nano Energy* **59** 138
[111] Davis J R 2001 *Copper and Copper Alloys* (ASM international) p 35
[112] Hoang H-M, Duong T-H, Tran N-H, Seo H, Kim J W, Kim J Y and Kim H C 2020 *Mater. Chem. Phys.* **246** 122852
[113] Fricoteaux P and Rousse C 2014 *J. Electroanal. Chem.* **733** 53
[114] Duong T H, Hoang H M and Kim H-C 2019 *AIP Conf. Proc.* **2083** 030003
[115] Hsieh Y-T, Tsai R-W, Su C-J and Sun I-W 2014 *J. Phys. Chem.* C **118** 22347
[116] Haberkorn N, Condó A M, Sirena M, Soldera F and Lovey F C 2014 *Mater. Lett.* **124** 256
[117] Chen Z, Ye S, Stewart I E and Wiley B J 2014 *ACS Nano* **8** 9673
[118] Meng N, Ma X, Wang C, Wang Y, Yang R, Shao J, Huang Y, Xu Y, Zhang B and Yu Y 2022 *ACS Nano* **16** 9095
[119] Hsu P-C, Wu H, Carney T J, McDowell M T, Yang Y, Garnett E C, Li M, Hu L and Cui Y 2012 *ACS Nano* **6** 5150
[120] Sannicolo T, Lagrange M, Cabos A, Celle C, Simonato P and Bellet D 2016 *Small* **12** 6052
[121] Zhang R and Engholm M 2018 *Nanomater.* **8** 628
[122] Crêpellière J, Menguelti K, Wack S, Bouton O, Mathieu G, Petru L P, Bianca R P, Renaud L and Michel M 2021 *ACS Appl. Nano Mater.* **4** 1126
[123] Akter T and Kim W S 2012 *ACS Appl. Mater. Interfaces* **4** 1855
[124] Kim T, Canlier A, Kim G H, Choi J, Park M and Han S M 2013 *ACS Appl. Mater. Interfaces* **5** 788
[125] Scardaci V, Coull R, Lyons P E, Rickard D and Coleman J N 2011 *Small* **7** 2621
[126] Zhao S, Han F, Li J, Meng X, Huang W, Cao D, Zhang G, Sun R and Wong P 2018 *Small* **14** 1800047
[127] Langley D, Giusti G, Mayousse C, Celle C, Bellet D and Simonato J-P 2013 *Nanotechnology* **24** 452001
[128] Chuan Fei Guo and Ren Z 2015 *Mater. Today* **18** 143
[129] Jung H P *et al* 2017 *Adv. Funct. Mater.* **27** 1701138
[130] Han S *et al* 2014 *Adv. Mater.* **26** 5808
[131] Wang Q, Abdallah N, Loffreda D, Ricolleau C, Alloyeau D, Louis C, Delannoy L, Jaysen N and Hazar G 2023 *Faraday Discuss.* **242** 375
[132] Honglin L and Chen X 2022 *Nanoscale* **14** 6688
[133] Jiang Y, Salley D, Sharma A, Keenan G, Mullin M and Cronin L 2022 *Sci. Adv.* **8** eabo2626